Inorg. Chem. **2006**, *45*, 3639–3647

Equatorially Connected Diruthenium(II,III) Units toward Paramagnetic Supramolecular Structures with Singular Magnetic Properties†

M. Carmen Barral,‡ Teresa Gallo,‡ Santiago Herrero,‡ Reyes Jiménez-Aparicio,*,‡ M. Rosario Torres,§ and Francisco A. Urbanos‡

Departamento de Química Inorgánica and Centro de Asistencia a la Investigación de Rayos X, Facultad de Ciencias Químicas, Universidad Complutense de Madrid, Ciudad Universitaria, 28040 Madrid, Spain

Received December 22, 2005

The reaction of $Ru_2Cl(O_2CMe)(DPhF)_3$ (DPhF = *N,N′*-diphenylformamidinate) with mono- and polycarboxylic acids gives a clean substitution of the acetate ligand, leading to the formation of complexes $Ru_2Cl(O_2CC_6H_5)(DPhF)_3$ (**1**), $Ru_2Cl(O_2CC_6H_4$-*p*-$CN)(DPhF)_3$ (**2**), $[Ru_2Cl(DPhF)_3(H_2O)]_2(O_2C)_2$ (**3**), $[Ru_2Cl(DPhF)_3]_2[C_6H_4$-*p*-$(CO_2)_2]$ (**4**), and $[Ru_2Cl(DPhF)_3]_3[C_6H_3$-1,3,5-$(CO_2)_3]$ (**5**). The preparation of $[Ru_2(NCS)(DPhF)_3]_3[C_6H_3$-1,3,5-$(CO_2)_3]$ (**6**) and $\{[Ru_2(DPhF)_3(H_2O)]_3[C_6H_3$-1,3,5-$(CO_2)_3]\}(SO_3CF_3)_3$ (**7**) from **5** is also described. All complexes are characterized by elemental analysis, IR and electronic spectroscopy, mass spectrometry, cyclic voltammetry, and variable-temperature magnetic measurements. The crystal structure determinations of complexes **2**·0.5THF and **3**·THF·$4H_2O$ (THF = tetrahydrofuran) are reported. The reactions carried out demonstrate the high chemical stability of the fragment $[Ru_2(DPhF)_3]^{2+}$, which is preserved in all tested experimental conditions. The stability of this fragment is also corroborated by the mass spectra. Electrochemical measurements reveal in all complexes one redox process due to the equilibrium $Ru_2^{5+} \leftrightarrow Ru_2^{6+}$. In the polynuclear complex **7**, some additional oxidation processes are also observed that have been ascribed to the presence of two types of dimetallic units rather than two consecutive reversible oxidations. The magnetic behavior toward temperature for complexes **1**–**7** from 300 to 2 K is analyzed. Complexes **1**–**7** show low values of antiferromagnetic coupling in accordance with the molecular nature in **1** and **2** and the absence of important antiferromagnetic interaction through the carboxylate bridging ligands in **3**–**7**, respectively. In addition, the magnetic properties of complex **7** do not correspond to any magnetic behavior described for diruthenium(II,III) complexes. The experimental data of compound **7** are simulated considering a physical mixture of $S = {}^1/_2$ and ${}^3/_2$ spin states. This magnetic study demonstrates the high sensitivity of the electronic configuration of the unit $[Ru_2(DPhF)_3]^{2+}$ to small changes in the nature of the axial ligands. Finally, the energy gap between the π^* and δ^* orbitals in these types of compounds allows the tentative assignment of the transition $\pi^* \rightarrow \delta^*$.

Introduction

The construction of supramolecular assemblies using metal−metal multiple-bonded complexes as building blocks represents an interesting research area with a great deal of potential for the design of molecular materials.[1−3] Thus, oligomers and polymers can be obtained by linking dimetallic units by axial or equatorial ligands.[4−7] A very useful

† Dedicated to Professor Rafael Usón on the occasion of his 80th birthday for his outstanding contribution to inorganic chemistry.

* To whom correspondence should be addressed. E-mail: qcmm@quim.ucm.es. Fax: 34 91 3944352.

‡ Departamento de Química Inorgánica.

§ Centro de Asistencia a la Investigación de Rayos X.

(1) (a) Ying, J.-W.; Sobransingh, D. R.; Xu, G.-L.; Kaifer, A. E.; Ren, T. *Chem. Commun.* **2005**, 357. (b) Hurst, S. K.; Ren, T. *J. Organomet. Chem.* **2003**, *670*, 188. (c) Ren, T.; Xu, G. L. *Comments Inorg. Chem.* **2002**, *23*, 355.

(2) (a) Cotton, F. A.; Lin, C.; Murillo, C. A. *Proc. Natl. Acad. Sci. U.S.A.* **2002**, *99*, 4810. (b) Cotton, F. A.; Lin, C.; Murillo, C. A. *Acc. Chem. Res.* **2001**, *34*, 759.

(3) (a) Chisholm, M. H.; Macintosh, A. M. *Chem. Rev.* **2005**, *105*, 2949. (b) Bursten, B. E.; Chisholm, M. H.; D'Acchioli, J. S. *Inorg. Chem.* **2005**, *44*, 5571. (c) Chisholm, M. H. *Acc. Chem. Res.* **2000**, *33*, 53.

(4) For example, see: (a) Cotton, F. A.; Murillo, C. A.; Yu, R. *Inorg. Chem.* **2005**, *44*, 8211. (b) Cotton, F. A.; Donahue, J. P.; Murillo, C. A.; Yu, R. *Inorg. Chim. Acta* **2005**, *358*, 1373. (c) Cotton, F. A.; Murillo, C. A.; Wang, X.; Yu, R. *Inorg. Chem.* **2004**, *43*, 8394. (d) Berry, J. F.; Cotton, F. A.; Ibragimov, S. A.; Murillo, F. A.; Wang, X. *Dalton Trans.* **2003**, 4297. (e) Cotton, F. A.; Dikarev, E. V.; Petrukhina, M. A.; Schmitz, M.; Stang, P. J. *Inorg. Chem.* **2002**, *41*, 2903.

10.1021/ic052174t CCC: $33.50
Published on Web 04/04/2006

structural motif in the construction of supramolecules is the unit $M_2(DArF)_3$, where DArF is *N*,*N*′-diarylformamidinate. Several polynuclear molybdenum complexes using the unit $[Mo_2(DArF)_3]^+$ and different linkers have been prepared.[8] Besides, a rich variety of architectures have been obtained using polycarboxylic acids such as 1,4-benzenedicarboxylic or 1,3,5-benzenetricarboxylic acids.[9]

Diruthenium compounds with a paddlewheel structure are especially interesting thanks to their electronic configuration and potential use as magnets, or other molecular devices.[10−12] The units $[Ru_2(L-L)_4]^+$ can be linked through their axial positions by a variety of anionic or neutral ligands providing polymeric arrangements.[10,11] However, the formation of supramolecular assemblies through the equatorial sites is very restricted because of the difficulty of preparing partially substituted diruthenium complexes. Thus, compounds with the composition $[Ru_2(O_2CR)_x(L-L)_{4-x}]^+$ (L−L = mononegative three-atom bridging ligand) are scarce,[12a,b,13−18] and supramolecular structures formed by diruthenium units bonded through equatorial positions are unusual. Recently,[17a] we have described the synthesis in high yield of the tris(formamidinato)diruthenium(II,III) complex $Ru_2Cl(O_2CMe)(DPhF)_3$ (DPhF = *N*,*N*′-diphenylformamidinate). This compound substitutes selectively the acetate ligand by other carboxylates and, therefore, is a good synthon for the preparation of supramolecular species. A similar complex $Ru_2Cl(O_2CMe)(DAniF)_3$ (DAniF = *N*,*N*′-*p*-anisydylformamidinate) has also been reported.[18]

In this paper, we describe the reaction of $Ru_2Cl(O_2CMe)(DPhF)_3$ with mono-, di-, and tricarboxylic acids in order to replace the acetate by other carboxylate groups to form supramolecular structures.

Table 1. Normal Modes of Vibration (NMV) of the Bridging Ligand DPhF Observed in the IR Spectra of Compounds **1**−**7**[a]

$\bar{\nu}$ (cm^{-1})	NMV	$\bar{\nu}$ (cm^{-1})	NMV	$\bar{\nu}$ (cm^{-1})	NMV
3058	$\nu(C-H)_{ar}$	1450	$\nu(C-C)_{ar}$	1027	$\delta_{ip}(C=C-H)_{ar}$
3032	$\nu(C-H)_{ar}$	1321	$\nu(C-N)$	960	$\delta(N=C-H)^b$
2958	$\nu(C-H)_{al}$	1219	$\nu(C-N)$	939	$\delta(N=C-H)^b$
1593	$\nu(C-C)_{ar}$	1177	$\delta_{ip}(C=C-H)_{ar}$	777	$\delta(C=N-C_{Ph})^b$
1534	$\nu(C=N)$	1155	$\delta_{ip}(C=C-H)_{ar}$	757	$\delta_{oop}(C=C-H)_{ar}$
1487	$\nu(C=N)$	1076	$\delta_{ip}(C=C-H)_{ar}$	626	$\delta_{oop}(C=C-H)_{ar}$

[a] The maximum deviation is 4 cm^{-1}. [b] Tentative assignments.

Results and Discussion

The reaction of $Ru_2Cl(O_2CMe)(DPhF)_3$ with benzoic or *p*-cyanobenzoic acids in refluxing methanol gives $Ru_2Cl(O_2CC_6H_5)(DPhF)_3$ (**1**) and $Ru_2Cl(O_2CC_6H_4$-*p*-$CN)(DPhF)_3$ (**2**), respectively. Similar reactions using oxalic, 1,4-benzenedicarboxylic, or 1,3,5-benzenetricarboxylic acids lead to the polynuclear compounds $[Ru_2Cl(DPhF)_3(H_2O)]_2(O_2C)_2$ (**3**), $[Ru_2Cl(DPhF)_3]_2[C_6H_4$-*p*-$(CO_2)_2]$ (**4**), and $[Ru_2Cl(DPhF)_3]_3[C_6H_3$-1,3,5-$(CO_2)_3]$ (**5**), respectively. In all cases, the acetate ligand is selectively substituted. The higher acidity and lower volatility of the carboxylic acids used in comparison with the acetic acid facilitate a clean substitution of the equatorial acetate ligand. In any case, the reactivity of $Ru_2Cl(O_2CMe)(DPhF)_3$ shows the chemical stability of the fragment $[Ru_2(DPhF)_3]^{2+}$. Complexes **2** and **4**−**7** are obtained as different solvates depending on the isolation procedure.

Similarly to other chlorodiruthenium(II,III) derivatives, the reaction of **5** with silver salts promotes the abstraction of the chloride axial ligand. Thus, the reactions with AgSCN or $AgSO_3CF_3$ lead to the complexes $[Ru_2(NCS)(DPhF)_3]_3[C_6H_3$-1,3,5-$(CO_2)_3]$ (**6**) and $\{[Ru_2(DPhF)_3(H_2O)]_3[C_6H_3$-1,3,5-$(CO_2)_3]\}(SO_3CF_3)_3$ (**7**), respectively. Complexes **1**−**7** are air stable even in solution for a large period of time and can be used to build structures with higher complexity, particularly **7**, which contains very labile ligands at the axial positions.

(5) Bera, J. K.; Bacsa, J.; Smucker, B. W.; Dunbar, K. R. *Eur. J. Inorg. Chem.* **2004**, 368.
(6) Takazaki, Y.; Yang, Z.; Ebihara, M.; Inoue, K.; Kawamura, T. *Chem. Lett.* **2003**, *32*, 120.
(7) (a) Xue, W. M.; Kühn, F. E. *Eur. J. Inorg. Chem.* **2001**, 2041. (b) Xue, W. M.; Kühn, F. E.; Herdtweck, E.; Li, Q. *Eur. J. Inorg. Chem.* **2001**, 213.
(8) For example, see: (a) Cotton, F. A.; de Meijere, A.; Murillo, C. A.; Rauch, K.; Yu, R. *Polyhedron* **2006**, *25*, 219. (b) Cotton, F. A.; Liu, C. Y.; Murillo, C. A.; Villagrán, D.; Wang, X. *J. Am. Chem. Soc.* **2004**, *126*, 14822. (c) Cotton, F. A.; Donahue, J. P.; Murillo, C. A.; Perez, L. M.; Yu, R. *J. Am. Chem. Soc.* **2003**, *125*, 8900. (d) Cotton, F. A.; Daniels, L. M.; Donahue, J. P.; Liu, C. Y.; Murillo, C. A. *Inorg. Chem.* **2002**, *41*, 1354.
(9) For example, see: (a) Stepanow, S.; Lingenfelder, M.; Dmitriev, A.; Spillmann, H.; Delvigne, E.; Lin, N.; Deng, X.; Cai, C.; Barth, J. V.; Kern, K. *Nat. Mater.* **2004**, *3*, 229. (b) Lingenfelder, M. A.; Spillmann, H.; Dmitriev, A.; Stepanow, S.; Lin, N.; Barth, J. V.; Kern, K. *Chem. Eur. J.* **2004**, *10*, 1913. (c) Angaridis, P.; Berry, J. F.; Cotton, F. A.; Murillo, C. A.; Wang, X. *J. Am. Chem. Soc.* **2003**, *125*, 10327. (d) Yang, L.; Naruke, H.; Yamase, T. *Inorg. Chem. Commun.* **2003**, *6*, 1020. (e) Lin, N.; Dmitriev, A.; Weckesser, J.; Barth, J. V.; Kern, K. *Angew. Chem., Int. Ed.* **2002**, *41*, 4779.
(10) (a) Cotton, F. A.; Walton, R. A. *Multiple Bonds between Metal Atoms*, 2nd ed.; Oxford University Press: Oxford, U.K., 1993. (b) Cotton, F. A., Murillo, C. A., Walton, R. A., Eds. *Multiple Bonds between Metal Atoms*, 3rd ed.; Springer Science and Business Media Inc.; New York, 2005.
(11) (a) Aquino, M. A. S. *Coord. Chem. Rev.* **1998**, *170*, 141. (b) Aquino, M. A. S. *Coord. Chem. Rev.* **2004**, *248*, 1025.
(12) For example, see: (a) Barral, M. C.; Herrero, S.; Jiménez-Aparicio, R.; Torres, M. R.; Urbanos, F. A. *Angew. Chem., Int. Ed.* **2005**, *44*, 305. (b) Angaridis, P.; Cotton, F. A.; Murillo, C. A.; Villagrán, D.; Wang, X. *J. Am. Chem. Soc.* **2005**, *127*, 5008. (c) Ren, T. *Organometallics* **2005**, *24*, 4854. (d) Vos, T. E.; Miller, J. S. *Angew. Chem., Int. Ed.* **2005**, *44*, 2416. (e) Vos, T. E.; Liao, Y.; Shum, W. W.; Her, J. H.; Stephens, P. W.; Reiff, W. M.; Miller, J. S. *J. Am. Chem. Soc.* **2004**, *126*, 11630. (f) Shi, Y.; Yee, G. T.; Wang, G.; Ren, T. *J. Am. Chem. Soc.* **2004**, *126*, 10552.
(13) (a) Angaridis, P.; Cotton, F. A.; Murillo, C. A.; Villagrán, D.; Wang, X. *Inorg. Chem.* **2004**, *43*, 8290. (b) Angaridis, P.; Berry, J. F.; Cotton, F. A.; Murillo, C. A.; Wang, X. *J. Am. Chem. Soc.* **2003**, *125*, 10327. (c) Cotton, F. A.; Yokochi, A. *Inorg. Chem.* **1998**, *37*, 2723. (d) Chakravarty, A. R.; Tocher, D. A.; Cotton, F. A. *Inorg. Chem.* **1985**, *24*, 2857. (e) Chakravarty, A. R.; Cotton, F. A. *Inorg. Chim. Acta* **1985**, *105*, 19.
(14) (a) Chen, W.-Z.; Ren. T. *Organometallics* **2005**, *24*, 2660. (b) Chen, W.-Z.; Ren, T. *Organometallics* **2004**, *23*, 3766. (c) Ren, T.; DeSilva, V.; Zou, G.; Lin, C.; Daniels, L. M.; Campana, C. F.; Alvarez, J. C. *Inorg. Chem. Commun.* **1999**, *2*, 301.
(15) Kachi-Terajima, C.; Miyasaka, H.; Ishii, T.; Sugiura, K.; Yamashita, M. *Inorg. Chim. Acta* **2002**, *332*, 210.
(16) Collin, J.-P.; Jouati, A.; Sauvage, J.-P.; Kaska, W. C.; McLoughlin, M. A.; Keder, N. L.; Harrison, W. T. A.; Stucky, G. D. *Inorg. Chem.* **1990**, *29*, 2238.
(17) (a) Barral, M. C.; Herrero, S.; Jiménez-Aparicio, R.; Torres, M. R.; Urbanos, F. A. *Inorg. Chem. Commun.* **2004**, *7*, 42. (b) Barral, M. C.; González-Prieto, R.; Herrero, S.; Jiménez-Aparicio, R.; Priego, J. L.; Royer, E. C.; Torres, M. R.; Urbanos, F. A. *Polyhedron* **2004**, *23*, 2637.
(18) Angaridis, P.; Berry, J. F.; Cotton, F. A.; Lei, P.; Lin, C.; Murillo, C. A.; Villagrán, D. *Inorg. Chem. Commun.* **2004**, *7*, 9.

Scheme 1. Proposed Ionization Pathway for Complex **7** According to the Fragments Detected in the ESI$^+$ MS and MS/MS Experiments

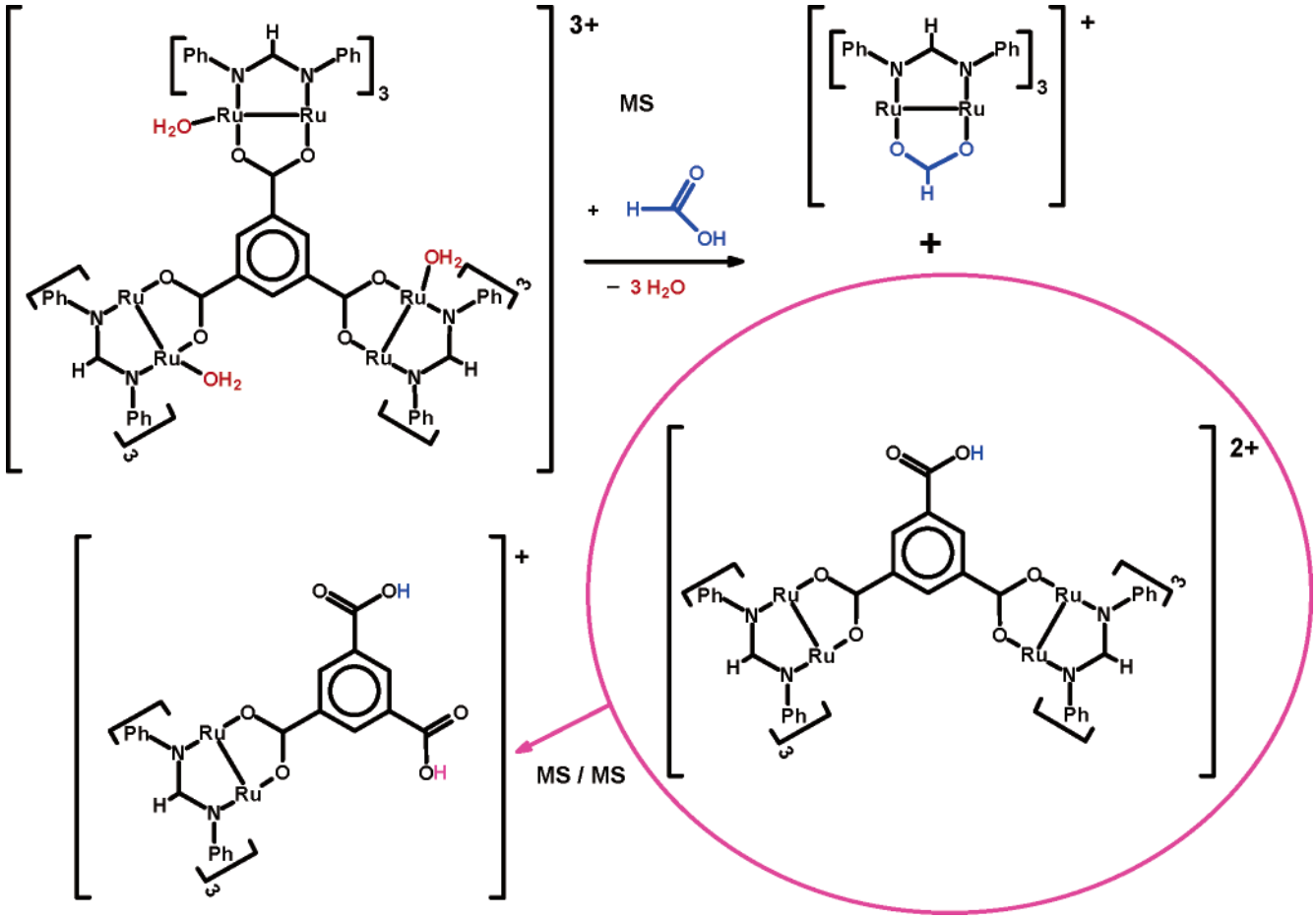

Table 2. Absorption Bands (cm^{-1}) for **1**−**7** Due to Groups Other Than DPhF

compd	ν(C≡N)	ν_a(COO)	ν_s(C−C)$_{ar}$	ν_s(COO)	δ(C═C−H)$_{ar}$
1		*a*		1408	
2	2229	1580		1409	860
3		1568		1317[b]	
4		*a*		1391	739
5		*a*	1449[b]	1371	733
6	2051	*a*	1449[b]	1372	734
7		*a*	1450[b]	1376	735

compd	ν_a(SO$_3$)	ν_s(CF$_3$)	ν_a(CF$_3$)	ν_s(SO$_3$)	δ_a(CF$_3$)	δ_s(SO$_3$)	δ_a(SO$_3$)
7	1281, 1261	1218[b]	1157[b]	1029[b]	757[b]	637	515

[a] Hidden by the ν(C−C)$_{ar}$ absorption. [b] Formamidinate ligands show bands by the same frequency (see Table 1).

IR Spectra. The characteristic bands due to the fragment $[Ru_2(DPhF)_3]^{2+}$ are preserved in the IR spectra of complexes **1**−**7** (Table 1). The ν_s(COO) absorption of the carboxylate group is shifted from 1432 cm^{-1} in the spectrum of the starting material[17a] to lower wavelengths for complexes **1**−**7**, respectively (Table 2). The corresponding band of the oxalato derivative (**3**) appears at 1317 cm^{-1}, together with one ν(C−N) absorption of the DPhF ligands.

The nitrile group of complex **2** absorbs at 2229 cm^{-1} (very weak), while the band of the SCN− group in **6** appears at 2051 cm^{-1} (very strong). The ν(CN) in complex **6** is very similar to the one observed[17b] for the isothiocyanato complex $Ru_2(NCS)(O_2CMe)(DPhF)_3$, which suggests the same N coordination of the SCN− ligand. Complex **7** shows characteristic bands of the triflate anion[19] (Table 2). Several of them appear at frequencies assigned to some normal modes of vibration of the DPhF$^-$ bridging ligands, which make them substantially more intense.

Mass Spectrometry (MS). The mass spectra of complexes **1**−**5** in chloroform show the peak corresponding to the fragment [M − axial ligand(s)]$^+$. However, for complex **1**, [M − Cl]$^+$ constitutes the base peak, whereas for complexes **2**−**5**, the base peak results from the loss of the axial ligands together with other fragments of the molecule. In the spectrum of complex **3**, the most intense peak (m/z = 834) is not well defined, surely owing to the sum of the fragments

(19) Johnston, D. H.; Shriver, D. F. *Inorg. Chem.* **1993**, *32*, 1045.

Table 3. Electrochemical Data (V) in CH_2Cl_2 of Complexes **1**−**7** and $Ru_2Cl(O_2CMe)(DPhF)_3$ (**a**), $Ru_2((NCS)(O_2CMe)(DPhF)_3$ (**b**), and $[Ru_2(O_2CMe)(DPhF)_3(H_2O)]BF_4$ (**c**)

complex	$E_{1/2}(A_1/A_1')$	ΔE	$E_{1/2}(A_2/A_2')$	ΔE	B_1'	B_2	B_2'
1	0.76	0.11			−0.62	−0.11	
a	0.74	0.10			−0.60	−0.15	
2	0.78	0.12	1.04	0.08	−0.56	−0.08	−0.12
3	0.80	0.16	1.08	0.08	−0.55	−0.07	
4	0.77	0.08	1.02	0.10	−0.58	−0.08	
5	0.77	0.10	0.95	0.08	−0.54	−0.08	
6[a]	0.85	0.20					
b	0.78	0.10			−0.50	−0.21	
7	0.79	0.11	1.00	0.10		−0.03	−0.20
c	0.74	0.07	0.99	0.05			

[a] Probably A_1 and A_2 processes are superimposed.

$\{[Ru_2(DPhF)_3]_2(O_2C)_2\}^{2+}$ ($M - 2Cl - 2H_2O$) and $[Ru_2(O_2CH)(DPhF)_3]^+$.

The mass spectra for complex **6** were obtained from a solution of the compound in chloroform that contained MeCN with formic acid (2%) to favor the ionization process. Only two peaks are observed between $m/z = 600$ and 3400 that fit with the fragments $[M - NCS]^+$ and $[M - 3NCS - H]^{2+}$, respectively.

Complex **7** gives in chloroform one peak with a value between $m/z = 2000$ and 3400 (at $m/z = 2577$), which is attributed to the loss of two triflate groups, a $DPhF^-$, and two H^+. The same compound in the presence of formic acid produces two intense peaks at $m/z = 835$ and 892 due to the fragments $[Ru_2(O_2CH)(DPhF)_3]^+$ and $\{[Ru_2(DPhF)_3]_2(O_2C)_2C_6H_3(COOH)\}^{2+}$, respectively. These two species are formed as a result of the reaction of **7** with a molecule of formic acid (Scheme 1). Also, both fragments should have about the same stability because they have similar intensities. Alternatively, the ion $\{[Ru_2(DPhF)_3]_2(O_2C)_2C_6H_3(COOH)\}^{2+}$ might be an impurity due to incomplete substitution in the preparation of complex **5**. However, in the MS/MS spectrum of **7**, the ion $\{[Ru_2(DPhF)_3]_2(O_2C)_2C_6H_3(COOH)\}^{2+}$ was selected, and the sole appreciable peak generated ($m/z > 600$) was attributed to the species $\{[Ru_2(DPhF)_3](O_2C)C_6H_3(COOH)_2\}^+$ ($m/z = 998$), which was not detected in the original spectrum. The same type of fragmentation, the loss of "$Ru_2(DPhF)_3$", is observed in the mass spectra of **4** in $CHCl_3$ (without formic acid), where the two more intense peaks are $[M - Cl]^+$ and $[M - Ru_2(DPhF)_3Cl]^+$ (100%).

The MS data corroborate the proposed stoichiometries for complexes **1**−**7** and as a whole indicate that the fragment $[Ru_2(DPhF)_3]^{2+}$ is quite stable.

Cyclic Voltammetry. The redox behavior of compounds **1**−**7** (Table 3) was investigated by cyclic voltammetry (CV). Complex **1** undergoes a well-defined redox process in CH_2Cl_2 (Figure 1) with an anodic potential of 0.82 V and a cathodic potential of 0.71 V owing to the reaction[9c,17a] $Ru_2^{5+} \leftrightarrow Ru_2^{6+}$. The irreversible processes observed at −0.62 and −0.11 V are attributed to the reduction $Ru_2^{5+} \rightarrow Ru_2^{4+}$, which is followed by the fast dissociation of the chloride ligand and ulterior oxidation of these last species ($Ru_2^{4+} \rightarrow Ru_2^{5+}$), as pointed out previously for other formamidinatodiruthenium(II,III) complexes.[20] These electrode reactions are labeled

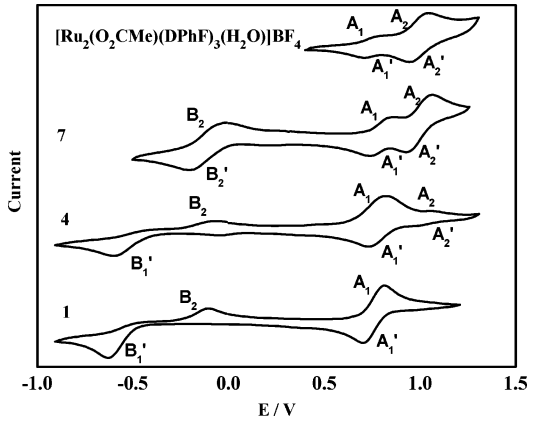

Figure 1. Cyclic voltammograms of complexes **1**, **4**, **7**, and $[Ru_2(O_2CMe)(DPhF)_3(H_2O)]BF_4$ in CH_2Cl_2 at 100 $mV \cdot s^{-1}$.

Scheme 2. Chemical and Electrochemical Processes Involved in the Redox Response of **1**−**5** (a) and **7** (b)

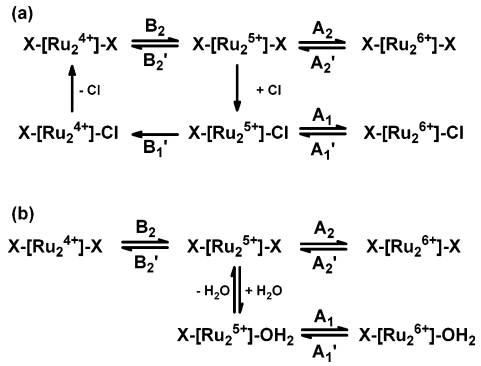

as processes A_1, B_1, and B_2 in Figure 1, Table 3, and Scheme 2a, where $X = BF_4^-$. The interaction of the BF_4^- group at the axial positions is favored by the high concentration of NBu_4BF_4 (0.1 M) present in the solution. Moreover, crystal structures of Ru_2^{5+} and Ru_2^{6+} with BF_4^- ligands at the axial positions have been described.[9c]

However, complex **7** shows two reversible redox processes (A_1 and A_2) at positive potentials and other processes at negative potentials (B_2) (Figure 1). The presence of two oxidation processes could be attributed to the existence of electronic communication across the trimesate ligand, as proposed for other polynuclear complexes formed by dimetallic units joined by trimesate groups.[21] However, analogous oxidation processes have also been observed for the complex $[Ru_2(O_2CMe)(DPhF)_3(H_2O)]BF_4$, where such electronic communication is not possible (Figure 1). Moreover, we discard the presence of two consecutive reversible oxidations $Ru_2^{5+} \rightarrow Ru_2^{6+} \rightarrow Ru_2^{7+}$, similar to those described for the complex $Ru_2(L)_4Cl$ (L = substituted amino- or anilinopyridinates) because both signals have different intensities. Hence, those oxidation processes can be ascribed to the presence of two types of dimetallic units: "X−Ru−Ru−OH_2" and "X−Ru−Ru−X" (Scheme 2b). The equilibrium between both species

(20) (a) Bear, J. L.; Han, B.; Huang, S.; Kadish, K. M. *Inorg. Chem.* **1996**, *35*, 3012. (b) Lin, C.; Ren, T.; Valente, E. J.; Zubkowski, J. D.; Smith, E. T. *Chem. Lett.* **1997**, 753.

(21) (a) Cotton, F. A.; Lu, J.; Yokochi, A. *Inorg. Chim. Acta* **1998**, *275*, 447. (b) Xu, G.-L.; Jablonski, C. G.; Ren, T. *Inorg. Chim. Acta* **2003**, *343*, 387.

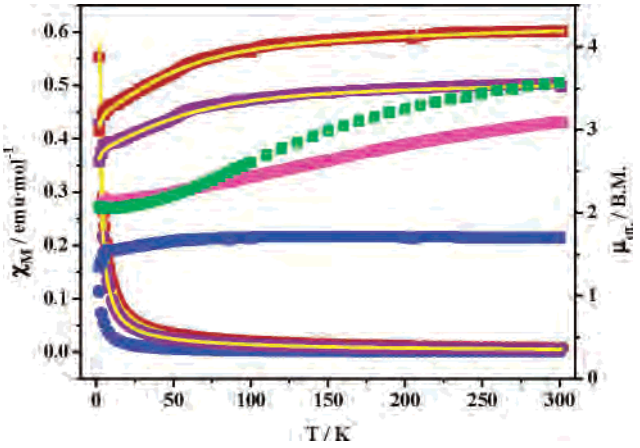

Figure 2. Magnetic susceptibility (●) and moment (■) vs temperature for the high-spin complex **1** (red ● ■), the low-spin $Ru_2(NCS)(O_2CMe)(DPhF)_3$ (blue ● ■), the physical spin mixture **7** (purple ● ■), the spin admixture $[Ru_2(O_2CMe)(DPhF)_3(H_2O)]BF_4$ (pink ■), and the Boltzmann distribution $Ru_2Cl(p\text{-}DAniF)_4$ (green ■). The solid lines are the result of the fitting of the experimental data as described in the text.

is more displaced to the nonaqueous form in the parent compound $[Ru_2(O_2CMe)(DPhF)_3(H_2O)]BF_4$, where the more basic character of the acetate ligand increases the lability of the water axial ligand.

Complex **6** shows a voltammogram comparable to that observed for **1** at positive values, but no electrochemical process for negative potentials until −1.5 V is perceived. Its value, 0.85 V, is intermediate between the values obtained for A_1 and A_2 reactions in other compounds and could correspond to the superimposition of both processes. The electrochemical behavior of the high-spin complex **6** contrasts with that observed for the low-spin complex $Ru_2(NCS)(O_2CMe)(DPhF)_3$, which does present a redox reaction at negative values. Again, the donor character of carboxylate ligands probably causes the difference.

Finally, complexes **2**−**5** show the same processes as that described for **1**, but in addition they show other anodic and cathodic signals with low intensities. These extra redox signals can be attributed to the existence of more species in equilibrium because of the higher electronegativity of the carboxylate group and the residual presence of water. In Figure 1, the voltammogram of complex **4** is depicted as an example.

Magnetic Properties. The magnetic moment at room temperature of complexes **1**−**6** (3.91−4.45 μ_B) corresponds to the presence of three unpaired electrons per dimetallic unit, as expected for the ground-state configuration[22] $\sigma^2\pi^4\delta^2(\pi^*\delta^*)^3$.

In all cases, the molar magnetic susceptibility increases from 300 to 2 K. The plot of μ_{eff} vs temperature (Figure 2) exhibits the typical slope previously observed in molecular or zigzag chain polymeric tetracarboxylatodiruthenium(II,III) complexes.[23−26] The decrease of the magnetic moment with a lowering of the temperature has been simulated with a previously described model,[25,26] where an important zero-field splitting and a small intermolecular antiferromagnetic interaction are considered. In addition, this model considers correction terms for temperature-independent paramagnetism (TIP) and a small amount of paramagnetic impurity (*P*). A very good agreement between the experimental and calculated curves of both the magnetic moment and the molar susceptibility for complexes **1**−**6** is obtained by using this model. Figure 2 shows the experimental and calculated magnetic data for **1** as an example. Table 4 collects the calculated magnetic parameters (*g*, *D*, *zJ*, TIP, and *P*) for these complexes. The *D* values (58.09−69.76 cm^{-1}) are similar to those found for tetracarboxylato complexes.[23−26]

The *zJ* values vary from −0.01 to −0.96 cm^{-1}. These low values could be anticipated for complexes **1** and **2**, where only a through-space antiferromagnetic interaction is possible between the diruthenium species.[26] However, for complexes **3**−**7**, an antiferromagnetic coupling might occur through the polycarboxylate ligand that bridges the dimetallic units. The low *zJ* values in compounds **4**−**6** indicate that neither 1,4-benzenedicarboxylate nor 1,3,5-benzenetricarboxylate ligands promote the magnetic interactions between the diruthenium units. However, the *zJ* value of −0.96 cm^{-1} in the oxalate complex **3** is slightly higher, which could be indicative of a better magnetic communication through this ligand.

The presence of three unpaired electrons per dimer unit in complex **6** contrasts with that observed[17b] in the related $Ru_2(NCS)(O_2CMe)(DPhF)_3$ complex, which has only one unpaired electron. The replacement of Cl^- by SCN^- in $Ru_2Cl(O_2CMe)(DPhF)_3$ produces a change of the spin configuration, whereas the high-spin configuration is retained after the same substitution in **5** to form **6**. This fact corroborates that in the compounds $Ru_2X(O_2CR)(DPhF)_3$ high- and low-spin configurations are very close in energy and small changes not only in the axial[12a,17b] but also in the equatorial ligand (carboxylate) can modify drastically their magnetic behavior.

The magnetic properties of complex **7** do not correspond to any magnetic behavior described for diruthenium(II,III) complexes: high spin (three unpaired electrons),[11] low spin (one unpaired electron),[17b] quantum mechanical spin admixed,[12a] or Boltzmann distribution[12b] between π^{*3} and $\pi^{*2}\delta^*$ electronic configurations. The magnetic moment at room temperature (3.52 μ_B) is intermediate between those corresponding to one and three unpaired electrons. However, the variation of the magnetic moment with temperature (from 3.52 μ_B at 300 K to 2.62 μ_B at 2 K) shows a pattern completely different from those observed for compounds where spin admixed or Boltzmann distribution occurs. Figure 2 illustrates all types of magnetic behavior reported for Ru^{II}−

(22) Norman, G. J.; Renzoni, G. E.; Case, D. A. *J. Am. Chem. Soc.* **1979**, *101*, 5256.

(23) Cotton, F. A.; Pedersen, E. *Inorg. Chem.* **1975**, *14*, 388.
(24) Telser, J.; Drago, R. S. *Inorg. Chem.* **1984**, *23*, 3114.
(25) (a) Cukiernik, F. D.; Luneau, D.; Marchon, J. C.; Maldivi, P. *Inorg. Chem.* **1998**, *37*, 3698. (b) Estiú, G.; Cukiernik, F. D.; Maldivi, P.; Poizat, O. *Inorg. Chem.* **1999**, *38*, 3030.
(26) (a) Barral, M. C.; González-Prieto, R.; Jiménez-Aparicio, R.; Priego, J. L.; Torres, M. R.; Urbanos, F. A. *Eur. J. Inorg. Chem.* **2004**, 4491. (b) Barral, M. C.; González-Prieto, R.; Jiménez-Aparicio, R.; Priego, J. L.; Torres, M. R.; Urbanos, F. A. *Eur J. Inorg. Chem.* **2003**, 2339. (c) Barral, M. C.; Jiménez-Aparicio, R.; Pérez-Quintanilla, D.; Priego, J. L.; Royer, E. C.; Torres, M. R.; Urbanos, F. A. *Inorg. Chem.* **2000**, *39*, 65.

Table 4. Magnetic Parameters for Complexes **1**−**7** Obtained in the Fits to the Magnetic Moment as a Function of Temperature

		g	D (cm^{-1})	zJ (cm^{-1})	TIP (emu·mol^{-1})	P (%)	σ^2
1		2.12	63.57	−0.10	3.8×10^{-4}	1.02×10^{-10}	1.5×10^{-5}
2		2.15	63.56	−0.09	9.5×10^{-5}	2.71×10^{-10}	1.4×10^{-5}
3		2.06	69.76	−0.96	3.1×10^{-3}	5.82×10^{-3}	3.4×10^{-5}
4		2.06	58.09	−0.07	3.5×10^{-4}	3.56×10^{-9}	2.8×10^{-5}
5		2.07	60.02	−0.08	3.0×10^{-4}	1.35×10^{-9}	2.6×10^{-5}
6		2.04	46.03	−0.01	1.2×10^{-11}	2.98×10^{-9}	6.1×10^{-5}
7	$S = {}^1/_2$ (25%)	2.03		−1.13	2.0×10^{-4}		3.0×10^{-5}
	$S = {}^3/_2$ (75%)	2.01	69.06	−0.04			

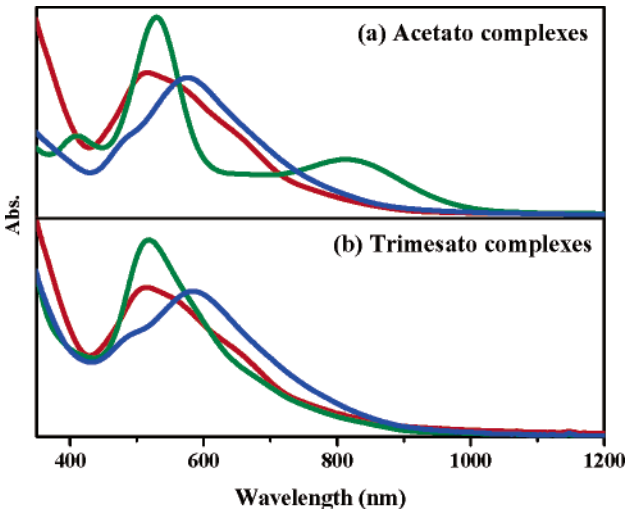

Figure 3. Absorption spectra in a CH_2Cl_2 solution of ca. 10^{-4} M of complexes (a) $Ru_2Cl(O_2CMe)(DPhF)_3$ (red line), $Ru_2(NCS)(O_2CMe)(DPhF)_3$ (green line), and $[Ru_2(O_2CMe)(DPhF)_3(H_2O)]BF_4$ (blue line) and (b) **5** (red line), **6** (green line), and **7** (blue line).

Ru^{III} complexes including the one referring to compound **7**. The susceptibility and magnetic moment curves of complex **7** have been simulated considering a physical mixture of $S = {}^1/_2$ and ${}^3/_2$ spin states. This model takes into account independent g and zJ values for each spin system together with zero-field splitting for the high-spin form and a global TIP term (see the Supporting Information). The experimental and calculated magnetic moment curves for **7** are depicted in Figure 2. The magnetic parameters obtained in the best fit are collected in Table 4.

Taking into account that there are three diruthenium units per molecule in complex **7**, the physical mixture could be due to the presence of one $S = {}^1/_2$ and two $S = {}^3/_2$ dimetallic units. However, it is known that a quantum spin admixture can be fitted as a physical mixture in some cases.[27] Thus, as a consequence of the closeness of low- and high-spin states in these types of complexes, the presence of a new case of spin admixed in **7** instead of a physical mixture cannot be discarded.

Electronic Properties. The visible spectra of the chloro complexes **1**−**5** display one maximum in the range 514−532 nm and two shoulders in the intervals 555−570 and 655−665 nm (Figure 3). The shapes and positions of the bands are comparable to those described for the complexes[20b] $Ru_2Cl(DArF)_4$ and have been ascribed to $\pi(Ru-N,Ru_2) \rightarrow \pi^*(Ru_2)$, $\pi^*(Ru_2) \rightarrow \sigma^*(Ru-N)$, and $\delta(Ru_2) \rightarrow \pi^*(Ru_2)$ transitions,[20b] respectively. Considering that the difference in energy between the π^* and δ^* orbitals must be similar to the electron pairing energy in these types of complexes,[12a,17b] an absorption band associated with the transition $\pi^* \rightarrow \delta^*$ should be expected in the visible region. Should the assignment of the above-mentioned bands be correct, the $\pi^* \rightarrow \delta^*$ transition must be clouded among the other absorptions.

The relative intensity of the bands is only slightly different for complex **6**, where the axial ligand is NCS^-. Assuming that the transition $\pi^* \rightarrow \delta^*$ absorbs in the visible range, the spectrum of the low-spin compound $Ru_2(NCS)(O_2CMe)(DPhF)_3$ should vary substantially. In fact, it contains three well-defined bands at 410, 529, and 812 nm and an almost imperceptible shoulder at 662 nm (Figure 3). To be a low-spin complex, the energy gap between π^* and δ^* levels must increase with respect to the high-spin complexes. Because complex $Ru_2(NCS)(O_2CMe)(DPhF)_3$ presents only one band in the visible region at higher energy (410 nm), we attribute this band to the $\pi^* \rightarrow \delta^*$ transition.

However, for complex **7**, two absorptions are detected: a shoulder at 492 nm and a maximum at 585 nm (Figure 3), similarly to the spectra of $[Ru_2(O_2CMe)(DPhF)_3(H_2O)]BF_4$ in CH_2Cl_2 or MeOH[12a] or $Ru_2(O_2CMe)(DPhF)_3Cl$ in MeOH[17a] (where the chloride acts as a counterion).

As described above, the magnetic behavior of complex **7** is explained as a physical spin mixture with a gap between the π^* and δ^* orbitals close to the pairing energy. For this compound, a shift to lower energy with respect to complex **6** could be expected for the $\pi^* \rightarrow \delta^*$ transition, and in accordance with this fact, the shoulder at 492 nm should be attributed to this transition.

X-ray Crystallography. Structure of $[Ru_2Cl(O_2CC_6H_4$-*p*-CN)$(DPhF)_3]\cdot 0.5THF$ (2·0.5THF) and $[Ru_2Cl(DPhF)_3(H_2O)]_2(O_2C)_2\cdot THF\cdot 4H_2O$ (3·THF·4H$_2$O) (THF = Tetrahydrofuran). Figures 4 and 5 show an ORTEP view of complexes **2**·0.5THF and **3**·THF·4H$_2$O, respectively. Selected bond lengths and angles for these complexes are collected in Table 5. The diruthenium units consist of almost eclipsed paddlewheel arrangements with three formamidinate and one carboxylate paddles in both complexes. The main feature in the structure of **3**·THF·4H$_2$O is the existence of two equivalent dimetallic units connected by an oxalate bridge group. The Ru−Ru distance in both complexes is similar to those observed for other trisformamidinato complexes.[17,18] The Ru−Cl bond distance is ∼0.05 Å longer in **3**·THF·4H$_2$O than in **2**·0.5THF and other $Ru_2Cl(O_2CR)(DPhF)_3$ compounds,[17a] probably because of the presence of

(27) Carney, M. J.; Papaefthymiou, G. C.; Spartalian, K.; Frankel, R. B.; Holm, R. H. *J. Am. Chem. Soc.* **1988**, *110*, 6084.

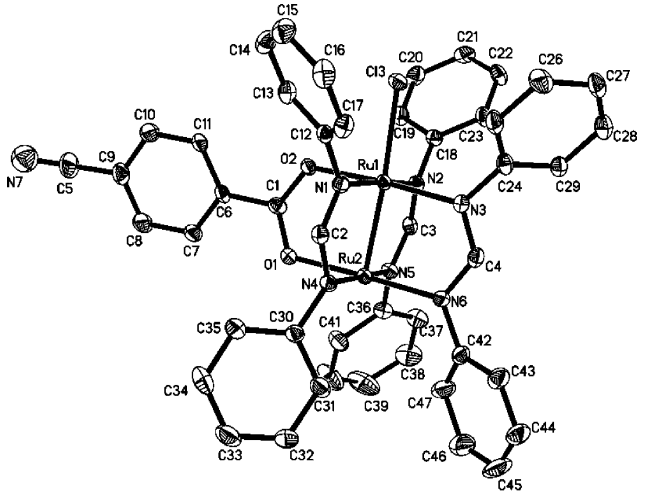

Figure 4. ORTEP view of **2**·0.5THF (thermal ellipsoids are shown at 30% probability). H atoms and crystallization solvent molecules are omitted for clarity.

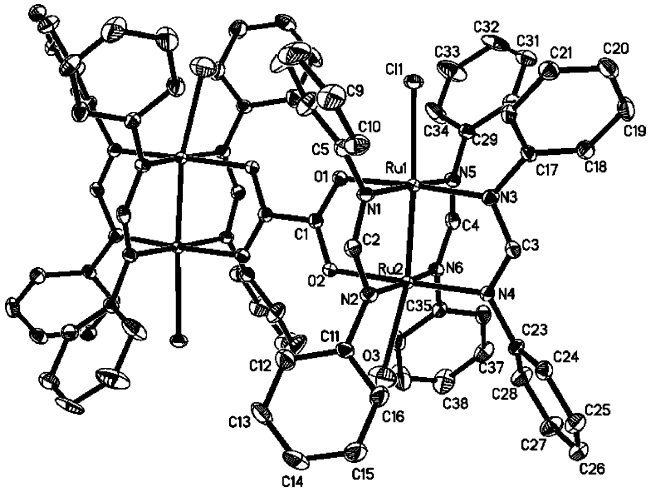

Figure 5. ORTEP view of **3**·THF·4H_2O (thermal ellipsoids are shown at 25% probability). H atoms and crystallization solvent molecules are omitted for clarity.

a water molecule coordinated at the other axial position. A lesser elongation of the Ru−Cl bond was observed[17a] in $Ru_2Cl(O_2CMe)(DPhF)_3$·HDPhF, where the chloride axial ligand is H-bonded to the formamidine of crystallization. In contrast with the complex **3**·THF·4H_2O, where both axial positions are occupied, in complex **2**·0.5THF, only one axial position of the dimetallic unit is occupied despite the presence of a terminal CN group in the carboxylate ligand. The CN group is also terminal in *cis*-$Rh_2(O_2CC_6H_4$-*p*-$CN)_2(DtolF)_2(py)_2$, the sole reported struc-ture where the *p*-cyanobenzoate ligand bridges two metals linked by a metal−metal bond.[28]

The only noteworthy short contact in **2**·0.5THF takes place through a $\pi-\pi$ interaction between the phenyl rings C30−C35 of two adjacent molecules located at 3.47(2) Å. However, in **3**·THF·4H_2O, although the H atoms of the water molecules have not been located, the O−O distances (3.000−2.769 Å) indicate the presence of several H bonds between these molecules and the O atoms from the oxalato group and the water axial ligands. In addition, the THF molecule is H-bonded to the axial water ligand. None of them links ruthenium complexes, which are packed only by van der Waals forces. This could be the reason these crystals of **3**·THF·4H_2O are dissolved faster than the solid isolated from the reaction (**3**), where the coordinated water and the chloride may bind adjacent molecules.

Table 5. Selected Bond Lengths (Å) and Angles (deg) for **2**·0.5THF and **3**·THF·4H_2O

2·0.5THF		**3**·THF·4H_2O	
Ru1−Ru2	2.3316(11)	Ru1−Ru2	2.3503(9)
Ru1−Cl3	2.407(3)	Ru1−Cl1	2.452(2)
		Ru2−O3	2.409(8)
Ru1−N av	2.079(8)	Ru1−N av	2.073(7)
Ru1−O2	2.091(6)	Ru1−O1	2.091(6)
Ru2−N av	2.035(8)	Ru2−N av	2.058(7)
Ru2−O1	2.062(6)	Ru2−O2	2.083(5)
Ru2−Ru1−Cl3	174.87(7)	Ru2−Ru1−Cl1	174.60(7)

Conclusions

The construction of supramolecular structures containing $[Ru_2(DPhF)_3]^{2+}$ units is possible by using the complex $Ru_2Cl(O_2CMe)(DPhF)_3$ thanks to the clean substitution of the acetate ligand by polycarboxylate groups. The presence of the fragment $[Ru_2(DPhF)_3]^{2+}$ in the derivatives is easily recognized by IR spectroscopy because it produces a set of characteristic bands. The mass spectra indicate a high stability of this fragment, and none of the complexes need to be kept under a protected atmosphere. The electrochemical studies show for some compounds the existence of several Ru_2^{5+} species in solution that can be oxidized to Ru_2^{6+} units, which are very scarce in carboxylato dimers of ruthenium. The change in the basic character of the carboxylate ligand and especially the nature of the axial ligand modifies drastically the gap energy between the π^* and δ^* orbitals, which leads not only to high- or low-spin configurations but also to intermediate situations such as quantum admixed or physical mixtures of $S = {}^1/_2$ and ${}^3/_2$ spin states. The tentative assignment of the transition $\pi^* \rightarrow \delta^*$ in the visible spectra could be useful to search for the existence of interesting magnetic properties in these types of compounds.

Experimental Section

General Remarks. Chemicals and solvents were purchased from commercial sources and used as received. $Ru_2Cl(O_2CMe)(DPhF)_3$,[17a] $Ru_2(NCS)(O_2CMe)(DPhF)_3$,[17b] $Ru_2(CN)(DPhF)_4$,[17b] and $[Ru_2(O_2CMe)(DPhF)_3(H_2O)]BF_4$[12a] were prepared by following published methods. The reactions with silver salts were carried out under exclusion of light. Elemental analyses were done by the Microanalytical Service of the Complutense University of Madrid. IR spectra were recorded on a Fourier transform Midac prospect spectrophotometer employing KBr pellets. Mass spectra were performed on a Bruker Esquire-LC with electrospray ionization. Nominal molecular masses and distribution isotopes of all peaks were calculated with the *MASAS*[29] computer program, using a polynomial expansion based on the natural abundances of the isotopes. Variable-temperature magnetic susceptibility measure-

(28) Lo Schiavo, S.; Nicolo F.; Tresoldi, G.; Piraino, P. *Inorg. Chim. Acta* **2003**, *343*, 351.

(29) Urbanos, F. A. *Program MASAS*, version 3.1; Universidad Complutense: Madrid, Spain, 2002.

Table 6. Crystallographic Data for **2**·0.5THF and **3**·THF·4H_2O

	2·0.5THF	**3**·THF·4H_2O
empirical formula	$C_{49}H_{41}ClN_7O_{2.5}Ru_2$	$C_{42}H_{37}ClN_6O_{5.5}Ru_2$
fw	1005.48	951.37
cryst syst	triclinic	triclinic
space group	$P\bar{1}$	$P\bar{1}$
a [Å]	12.9701(13)	13.3142(17)
b [Å]	13.8213(14)	14.4645(19)
c [Å]	16.7944(17)	14.967(2)
α [deg]	68.579(2)	94.827(2)
β [deg]	82.519(2)	115.420(2)
γ [deg]	66.935(2)	114.495(2)
V [Å^3]	2578.3(5)	2245.3(5)
Z	2	2
D_{calcd} [g·cm^{-3}]	1.295	1.407
μ [mm^{-1}]	0.680	0.780
F(000)	1018	960
cryst size [mm^3]	0.09 × 0.14 × 0.25	0.02 × 0.30 × 0.30
θ range [deg]	1.30−25.00	1.59−25.00
index ranges	$-14 \le h \le 15$ $-9 \le k \le 16$ $-19 \le l \le 19$	$-15 \le h \le 11$ $-17 \le k \le 17$ $-14 \le l \le 17$
collected reflns	13498	11755
independent reflns	8969 [R(int) = 0.0646]	7781 [R(int) = 0.0422]
completeness [%] to $\theta = 25°$	98.6	98.5
data/restraints/param	8969/5/547	7781/0/542
GOF on F^2	1.086	1.012
final R indices [$I > 2\sigma(I)$]	R1 = 0.0664, wR2 = 0.2297	R1 = 0.0553, wR2 = 0.1671
R indices (all data)	R1 = 0.1173, wR2 = 0.2547	R1 = 0.0994, wR2 = 0.1923
largest diff peak/hole [e·Å^{-3}]	1.544/−0.612	0.962/−0.630

ments were carried out on a Quantum Design MPMSXL SQUID magnetometer. All data were corrected for the diamagnetic contribution to the susceptibility of both the sample holder and the compound. The molar diamagnetic corrections for the complexes were calculated on the basis of Pascal's constants. The fittings of the experimental data were performed using the commercial *MATLAB* V.5.1.0.421 program. CV experiments were carried out with a potentiostat Pstat 10 Autolab Eco Chemie. A three-electrode system was used and consisted of a platinum disk working electrode, a platinum wire counter electrode, and a Ag|AgCl reference electrode (the potential of which is 0.140 V). The experiments were performed at room temperature under a nitrogen atmosphere, in CH_2Cl_2 solutions that contained 0.1 M NBu_4BF_4 as the supporting electrolyte, with a scan rate of 100 mV·s^{-1}. Electronic spectra of the complexes in a dichloromethane solution (~10^{-4} M) were acquired on a Cary 5G spectrophotometer.

Preparation of $Ru_2Cl(O_2CC_6H_5)(DPhF)_3$ (1). A mixture of $Ru_2Cl(O_2CMe)(DPhF)_3$ (0.207 g, 0.235 mmol), LiCl (0.100 g, 2.358 mmol), benzoic acid (0.034 g, 0.278 mmol), and methanol (10 mL) was refluxed for 4 h. The system was cooled to room temperature under a nitrogen flow. The violet solid was filtered, washed with methanol (2 × 3 mL) and diethyl ether (5 × 2 mL), and dried under vacuum. Yield: 0.179 g (81%). Anal. Found (calcd for $C_{46}H_{38}ClN_6O_2Ru_2$): C, 58.37 (58.50); H, 4.10 (4.06); N, 8.84 (8.90). MS-ESI in $CHCl_3$: m/z 910 ([M − Cl]$^+$, 100%). $\mu_{eff} = 4.19\ \mu_B$ at room temperature. Vis−NIR in CH_2Cl_2: λ_{max} (nm) 519, 566sh, 662sh.

Preparation of $[Ru_2Cl(O_2CC_6H_4$-p-$CN)(DPhF)_3]\cdot H_2O$ (2·H_2O). This compound was prepared similarly to **1** employing *p*-cyanobenzoic acid (0.101 g, 0.681 mmol). Yield: 0.517 g (77%). Anal. Found (calcd for $C_{47}H_{39}ClN_7O_3Ru_2$): C, 57.15 (57.17); H, 3.84 (3.98); N, 9.90 (9.93). MS-ESI in $CHCl_3$: m/z 909 ([M − Cl − CN]$^+$, 100%), 935 ([M − Cl]$^+$, 73%). $\mu_{eff} = 4.15\ \mu_B$ at room temperature. Vis−NIR in CH_2Cl_2: λ_{max} (nm) 524, 570sh, 659sh. Crystals of **2**·0.5THF suitable for X-ray analysis were formed by diffusion of hexane on a solution of compound **2** in THF.

Preparation of $[Ru_2Cl(DPhF)_3(H_2O)]_2(O_2C)_2$ (3). This complex was obtained following the same procedure as that described for **1** using $Ru_2Cl(O_2CMe)(DPhF)_3$ (0.205 g, 0.227 mmol) and oxalic acid dihydrate (0.014 g, 0.113 mmol) in a ratio of 2:1. Yield: 0.140 g (70%). Anal. Found (calcd for $C_{80}H_{70}Cl_2N_{12}O_6Ru_4$): C, 54.09 (54.27); H, 3.73 (3.98); N, 9.51 (9.49). MS-ESI in $CHCl_3$: m/z 1700 ([M − Cl]$^+$, 38%), 834 ([M − 2Cl]$^{2+}$ + [(M − 2Cl)/2 + H]$^+$, 100%). $\mu_{eff} = 4.45\ \mu_B$ per dimetallic unit at room temperature. Vis−NIR in CH_2Cl_2: λ_{max} (nm) 532, 565sh, 660sh. Crystals of **3**·THF·4H_2O were collected after a slow diffusion of hexanes over a THF solution of the complex.

Preparation of $[Ru_2Cl(DPhF)_3]_2[C_6H_4$-$p$-$(CO_2)_2]\cdot 0.5H_2O$ (4·0.5H_2O). This compound was prepared similarly to **1** employing terephthalic acid (0.019 g, 0.114 mmol). Yield: 0.181 g (87%). Anal. Found (calcd for $C_{86}H_{71}Cl_2N_{12}O_{4.5}Ru_4$): C, 56.75 (56.76); H, 3.92 (3.93); N, 9.24 (9.24). MS-ESI in $CHCl_3$: m/z 1776 ([M − Cl]$^+$, 45%), 987 ([M − $Ru_2(DPhF)_3Cl$]$^+$, 100%). $\mu_{eff} = 4.18\ \mu_B$ per dimetallic unit at room temperature. Vis−NIR in CH_2Cl_2: λ_{max} (nm) 519, 558sh, 658sh.

Preparation of $[Ru_2Cl(DPhF)_3]_3[C_6H_3$-1,3,5-$(CO_2)_3]\cdot H_2O$ (5·H_2O). This complex was synthesized following the same procedure as that described for **1** using $Ru_2Cl(O_2CMe)(DPhF)_3$ (0.200 g, 0.227 mmol) and trimesic acid (0.017 g, 0.076 mmol) in a ratio of 3:1. Yield: 0.141 g (69%). Anal. Found (calcd for $C_{126}H_{104}Cl_3N_{18}O_7Ru_6$): C, 56.22 (56.15); H, 3.85 (3.89); N, 9.34 (9.35). MS-ESI in $CHCl_3$: m/z 2644 ([M − Cl + 2H]$^+$, 100%), 1819 ([M − $Ru_2(DPhF)_3Cl_2$]$^+$, 77%). $\mu_{eff} = 4.10\ \mu_B$ per dimetallic unit at room temperature. Vis−NIR in CH_2Cl_2: λ_{max} (nm) 514, 558sh, 656sh.

Preparation of $[Ru_2(NCS)(DPhF)_3]_3[C_6H_3$-1,3,5-$(CO_2)_3]\cdot H_2O\cdot$THF (6·$H_2O$·THF). To a solution of **5**·H_2O (0.202 g, 0.071 mmol) in THF (15 mL) was added AgSCN (0.036 g, 0.216 mmol). The mixture was stirred for 1 day, and the resulting purple solution was filtered over Celite and layered with hexane to give the pure complex. Yield: 0.129 g (64%). Anal. Found (calcd for $C_{133}H_{112}N_{21}O_8Ru_6S_3$): C, 56.26 (56.35); H, 3.98 (3.98); N, 10.37 (10.37); S, 3.41 (3.39). MS-ESI in $CHCl_3$/MeCN, HCOOH 2%: m/z 2687

([M − NCS]$^+$), 1286 ([M − 3NCS + H]$^{2+}$). μ_{eff} = 3.91 μ_B per dimetallic unit at room temperature. Vis−NIR in CH_2Cl_2: λ_{max} (nm) 519, 589sh, 659sh.

Preparation of {$[Ru_2(DPhF)_3(H_2O)]_3(O_2C)_3C_6H_3$}$(SO_3CF_3)_3$·2THF (7·2THF). The preparation was carried out as described above for **6** using **5**·H_2O (0.202 g, 0.071 mmol) and $AgSO_3CF_3$ (0.055 g, 0.216 mmol) in a ratio of 1:3. Yield: 0.138 g (60%). Anal. Found (calcd for $C_{137}H_{124}F_9N_{18}O_{20}Ru_6S_3$): C, 51.04 (51.16); H, 3.92 (3.89); N, 7.73 (7.84); S, 2.67 (2.99). MS-ESI in $CHCl_3$: *m*/*z* 2579 ([M − $2SO_3CF_3$ − DPhF]$^+$), 834 ([$Ru_2(O_2CH)(DPhF)_3$]$^+$). MS-ESI in $CHCl_3$/MeCN, HCOOH 2%: *m*/*z* 834 ([$Ru_2(O_2CH)$-$(DPhF)_3$]$^+$, 100%), 892 ([M − $3SO_3CF_3$ − $3H_2O$ − $Ru_2(DPhF)_3$ + H]$^{2+}$, 90%). MS/MS of 892 (daughter scan): 998 {$Ru_2(DPhF)_3$-$[(O_2C)C_6H_3(CO_2H)_2H)_2]$}$^+$, 100%). μ_{eff} = 3.52 μ_B per dimetallic unit at room temperature. Vis−NIR in CH_2Cl_2: λ_{max} (nm) 492sh, 585.

X-ray Crystallographic Study. Details of the data collection and crystal structure refinement correction for **2**·0.5THF and **3**·THF·$4H_2O$ are summarized in Table 6. Representative crystals were mounted on a Bruker Smart CCD diffractometer with graphite-monochromated Mo Kα (λ = 0.71073 Å) radiation. Data were collected, at 293(2) K, over a hemisphere of the reciprocal space by a combination of three exposure sets. The cell parameters were refined by a least-squares fit of all reflections collected. The structures were solved by direct methods and refined by the full-matrix least-squares methods against F^2 of all data. Calculations were performed with the aid of the *SHELXS* and *SHELXL* programs.[30,31] Final mixed refinement for complex **2**·0.5THF was undertaken with anisotropic thermal parameters for the non-H atoms with the exception of the solvent molecule and the N atom of the cyano group, which were only isotropically refined. Complex **3**·THF·$4H_2O$ was anisotropically refined. After the last cycles of refinement for complex **2**·0.5THF, some electronic density was located at the Fourier difference, which was assigned to a solvent rest.

Acknowledgment. We are grateful to Prof. C. A. Murillo and Prof. F. A. Cotton for providing us the magnetic data of the complex $Ru_2Cl(p\text{-}DAniF)_4$. This research was supported by funds from the Spanish Ministry for Education and Science (Project Nos. MAT2004-22102-E and CTQ2005-00397/BQU).

Supporting Information Available: X-ray crystallographic data for **2**·0.5THF and **3**·THF·$4H_2O$ in CIF format and equations used in the fit of the magnetic moment and susceptibility of complex **7**. This material is available free of charge via the Internet at http://pubs.acs.org.

IC052174T

(30) Sheldrick, G. M. *SHELXS-97, Program for the Solution of Crystal Structures*; University of Götttingen: Götttingen, Germany, 1997.
(31) Sheldrick, G. M. *SHELXL-97, Program for the Solution of Crystal Structures*; University of Götttingen: Götttingen, Germany, 1997.